Alteration in Plasma Metabolome in High-Fat Diet-Fed Monocyte Chemotactic Protein-1 Knockout Mice Bearing Pulmonary Metastases of Lewis Lung Carcinoma

Nutrition and Metabolic Insights
Volume 15: 1–11

DOI: 10.1177/11786388221111126

Lin Yan, Bret M Rust, Sneha Sundaram, Matthew J Picklo and Michael R Bukowski

U.S. Department of Agriculture, Agricultural Research Service, Grand Forks Human Nutrition Research Center, Grand Forks, ND, USA.

ABSTRACT: Both clinical and laboratory studies have shown that monocyte chemotactic protein-1 (MCP-1) is involved in cancer spread. To understand the role of MCP-1 in metabolism in the presence of metastasis, we conducted an untargeted metabolomic analysis of primary metabolism on plasma collected from a study showing that MCP-1 deficiency reduces spontaneous metastasis of Lewis lung carcinoma (LLC) to the lungs in mice fed a high-fat diet (HFD). In a 2 × 2 design, wild-type (WT) or *Mcp-1* knockout (*Mcp-1*$^{-/-}$) mice maintained on the AIN93G standard diet or HFD were subcutaneously injected with LLC cells to induce lung metastasis. We identified 87 metabolites for metabolomic analysis from this study. Amino acid metabolism was altered considerably in the presence of LLC metastases with the aminoacyl-tRNA biosynthesis pathways as the leading pathway altered. The HFD modified lipid and energy metabolism, evidenced by lower contents of arachidonic acid, cholesterol, and long-chain saturated fatty acids and higher contents of glucose and pyruvic acid in mice fed the HFD. These findings were supported by network analysis showing alterations in fatty acid synthesis and glycolysis/gluconeogenesis pathways between the 2 diets. Furthermore, elevations of the citrate cycle intermediates (citric acid, fumaric acid, isocitric acid, and succinic acid) and glyceric acid in *Mcp-1*$^{-/-}$ mice, regardless of diet, suggest the involvement of MCP-1 in mitochondrial energy metabolism during LLC metastasis. The present study demonstrates that MCP-1 deficiency and the HFD altered plasma metabolome in mice bearing LLC metastases. These findings can be useful in understanding the impact of obesity on prevention and treatment of cancer metastasis.

KEYWORDS: Metabolome, plasma, MCP-1, metastasis, Lewis lung carcinoma, diet, mice

RECEIVED: March 16, 2022. **ACCEPTED:** June 15, 2022.

TYPE: Original Research Article

FUNDING: The author(s) disclosed receipt of the following financial support for the research, authorship, and/or publication of this article: This work was funded by the USDA Agricultural Research Service Projects 3062-51000-050-00D, 3062-51000-056-00D, and 3062-53000-001-00D.

DECLARATION OF CONFLICTING INTERESTS: The author(s) declared no potential conflicts of interest with respect to the research, authorship, and/or publication of this article.

CORRESPONDING AUTHOR: Lin Yan, U.S. Department of Agriculture, Agricultural Research Service, Grand Forks Human Nutrition Research Center, 2420 2nd Avenue North, Grand Forks, ND 58203, USA. Email: Lin.Yan@usda.gov

Introduction

Monocyte chemotactic protein-1 (MCP-1) is a member of the chemokine family.[1] Initially, MCP-1 was identified as a potent chemotactic factor for recruiting monocytes to the site of infection for tissue repair.[2] However, growing evidence has shown that MCP-1 is involved in various diseases including cancer.

An elevated expression of MCP-1 is related to malignant aggression in cancer patients. For example, an increase of MCP-1 in serum is associated with advanced tumor stage and lymph node involvement in breast cancer.[3] Elevated expression of MCP-1 is associated with advanced prostate cancer[4] and is related to colorectal metastasis to liver in colorectal cancer.[5] Findings from laboratory studies are consistent with and support these clinical observations. Silencing of *Mcp-1*[6] or stable *Mcp-1* knockout[7] reduces mammary tumorigenesis and metastasis in the MDA-MB-231 breast cancer model. Depletion of MCP-1 reduces mammary tumorigenesis of triple negative breast cancer[8] and spontaneous metastasis of Lewis lung carcinoma[9] in mice.

Adipose tissue produces many chemokines including MCP-1.[10,11] The expression of *MCP-1* gene is higher in adipose tissue of obese patients compared to lean controls.[10] Adipose MCP-1 production is positively correlated with body adiposity and body mass index.[12] Obesity is related to a greater risk of recurrence and poor prognosis in breast cancer[13,14] and prostate cancer patients[15,16] when compared to patients with normal body weights. Recent animal studies have shown that adipose-derived MCP-1 contributes to mammary tumorigenesis in MMTV-PyMT mice[17,18] and pulmonary metastasis of Lewis lung carcinoma in C57BL/6 mice.[19]

The MCP-1 is involved in metabolic homeostasis.[20-22] Malignant cancer demands high energy and nutrient uptake and accelerated anabolism and catabolism to satisfy its rapid progression. We reported that the high-fat diet enhances pulmonary metastasis from a subcutaneous tumor in mice, evidenced by increases in the number and size of metastases form in the lungs, and that *Mcp-1* knockout reduces the high-fat diet-enhanced spontaneous metastasis.[9] To understand the role of MCP-1 in metabolism in the presence of metastasis, we conducted an untargeted metabolomic analysis of primary metabolism on plasma samples collected from the aforementioned study showing that *Mcp-1* knockout reduces the high-fat diet-enhanced metastasis.[9]

Materials and Methods

Animals and diets

Four to five-week-old male *Mcp-1* knockout mice (*Mcp-1*$^{-/-}$, B6.129S4-*Ccl2*^{tm1Rol}/J) on a C57BL/6J background and C57BL/6J wild-type (WT) mice were purchased from

The Jackson Laboratory (Bar Harbor, ME, USA). Mice were housed in a pathogen-free room (light-dark cycle: 12/12 hours, room temperature: 22°C ± 1°C). A modified AIN93G formulation providing 16% or 45% of energy from corn oil (hereafter referred to as AIN93G diet or high-fat diet, HFD) was used in this study.[9] Mice had free access to their diets and deionized water; they were weighed weekly.

Lewis lung carcinoma cell line

The Lewis lung carcinoma (LLC) cell line[23] was obtained from Dr. Pnina Brodt (McGill University, Montreal, Quebec, Canada). The cells were cultured with RPMI-1640 medium supplemented with 10% heat-inactivated fetal bovine serum and maintained in a humidified atmosphere of 5% CO_2 in air at 37°C. Cells were free of mycoplasma (Hoechst DNA staining and direct culture tests performed by American Type Cell Collection, Manassas, VA, USA).

Experimental design

The Institutional Animal Care and Use Committee of the Grand Forks Human Nutrition Research Center approved this study. The procedures followed the National Institutes of Health Guidelines for the Care and Use of Laboratory Animals.[24]

The study design was previously reported.[9] Briefly, mice (n = 28 per group for WT mice, n = 21 per group for *Mcp-1*$^{-/-}$ mice) were fed the AIN93G diet or HFD for 7 weeks before they were subcutaneously injected with 2.5×10^5 LLC cells into the lower dorsal region. The resulting subcutaneous tumor was resected 11 days later when it was approximately 1 cm in diameter. All surgeries for the study were completed within 3 days. Mice were then maintained on their respective diets for additional 10 days. At termination, lungs were harvested to assess the extent of metastasis. Plasma was collected for biomarker and metabolomic analyses.

Metabolomic analysis

Twelve plasma samples from each WT group and 10 from each *Mcp-1*$^{-/-}$ group were randomly chosen for metabolomic analysis. The chosen sample size was restricted by the availability due to the use of plasma for biomarker analysis in the original publication.[9] The metabolomic analysis[25,26] was performed at the West Coast Metabolomics Center (University of California-Davis Genomic Center, Davis, CA, USA). Plasma samples were prepared by silylation methyloximation and analyzed by gas chromatography time-of-flight mass spectrometry (GC-TOF-MS) for untargeted metabolomics of primary metabolism. Obtained data were processed by the BinBase database at the West Coast Metabolomics Center (University of California-Davis Genomic Center).[27] Quantifier ion peak heights of the identified compounds were normalized to the sum intensities of all known compounds. Unidentified peaks as well as those representing less than 0.02% of total signal intensity were excluded from statistical analysis. Additional compounds were excluded if they could not be identified as metabolic intermediates or endpoints common to mammalian metabolism based on the Kyoto Encyclopedia of Genes and Genomes (KEGG) Database or the Human Metabolome Database.[28-30]

Statistical analyses

A 2-way analysis of variance was used to evaluate effects of diet (AIN93G vs. HFD), genotype (WT vs. *Mcp-1*$^{-/-}$), and their interactions on changes in plasma metabolites in mice bearing LLC metastases, with the false discovery rate-corrected *P* values reported. Values from treatment groups were normalized as fold changes in comparison to WT mice fed the AIN93G diet. Results are reported as means ± standard error of the mean (SEM). SAS 9.4 (SAS Institute, Cary, NC, USA) was used for the analyses. Differences with $P \leq .05$ are considered significant.

Metabolomic analyses were performed by using MetaboAnalyst 5.0 (McGill University, Sainte Anne de Bellevue, Quebec, Canada). Data were scaled by the Pareto scaling method and analyzed by the sparse partial least square-discriminant analysis (sPLS-DA).[31,32] The hierarchical clustering heatmap analysis was performed by using the normalized peak intensity with Euclidean distance for distance measurement and the Ward error sum of squares hierarchical clustering method for Cluster algorithm. Group averages for the 25 metabolites that differed most among the 4 groups were reported.

Pathway analysis of alterations in metabolic pathways by LLC metastasis was performed by using the pathway library for *Mus musculus* according to the KEGG database[33,34] (MetaboAnalyst 5.0, McGill University). Pathway enrichment analysis coupled with the pathway topology analysis was conducted to identify altered metabolic pathways, with the Holm-adjusted *P* values reported.[35] Network analysis was performed to map the functional relationships of the identified metabolites by using the KEGG global metabolic network analysis and the metabolite-metabolite interaction network analysis (MetaboAnalyst 5.0, McGill University). Differences with $P \leq .05$ are considered significant.

Results

Pulmonary metastasis

All mice subcutaneously injected with LLC cells form a primary tumor at the injection site and metastatic nodules in the lungs.[9] The *Mcp-1* knockout mitigates lung metastasis, evidenced by decreases in the number and size of metastases in the lungs.[9]

Metabolomic analysis

We identified 133 compounds (Supplemental Table 1) from 498 discrete signals determined by the GC-TOF-MS. Eighty-seven of these 133 compounds (Supplemental Table 2) met the criteria for statistical analysis. These 87 metabolites were categorized into 4 groups related to amino acid, energy, lipid, and vitamin and nucleotide metabolism and were presented in Tables 1 to 4, respectively. Thirty-six of these metabolites differed significantly among the 4 groups, including 27 between the AIN93G diet and HFD, 13 between WT and *Mcp-1*$^{-/-}$ mice, and one interaction between the genotype and diet (Tables 1–4).

The hierarchical clustering heatmap analysis provides intuitive visualization of the results. The 25 metabolites that differed most among the 4 dietary groups were grouped into 5 clusters (Figure 1). Cluster 1 included branched-chain amino acids (BCAA) valine and isoleucine which were higher in WT mice fed the AIN93G diet compared to other groups. Cluster 2 included myristic acid (14:0), 1,5-anhydroglucitol, palmitoleic acid (16:1), arachidonic acid (20:4), cholesterol, palmitic acid (16:0), and stearic acid (18:0). These metabolites were relatively higher in AIN93G-fed mice than in HFD-fed mice, particularly AIN93G-fed *Mcp-1*$^{-/-}$ mice. In cluster 3, nine metabolites were elevated in HFD-fed mice, regardless of genotype. These included allantoic acid, glucose, pseudouridine, glycine, pyruvic acid, myoinositol, serine, galactitol, and methyl O-D-galactopyranoside. In cluster 4, 3 metabolites (glyceric acid, citric acid, and succinic acid) were elevated in *Mcp-1*$^{-/-}$ mice, regardless of diet. In cluster 5, four metabolites fucose, sorbitol, ribose, and oxoproline were elevated in HFD-fed *Mcp-1*$^{-/-}$ mice compared to other groups. These findings showed that the HFD and *Mcp-1* knockout altered the expression of metabolites in mice bearing LLC metastases.

The sPLS-DA scores plot showed separation by the HFD and *Mcp-1* knockout among the 4 groups (Figure 2). Along the *x*-axis, component 1 showed a separation between the AIN93G diet and HFD (Figure 2A). Along the y-axis, component 2 showed a separation between WT and *Mcp-1*$^{-/-}$ mice fed the AIN93G diet, but not mice fed the HFD (Figure 2A).

The loadings plot showed the metabolites identified by the sPLS-DA model for components 1 and 2. The loadings plot for component 1 identified energy metabolites (1,5-anhydroglucitol, galacitol, glucose, methyl-O-D-galactopyranoside, myoinositol, and pyruvic acid) and fatty acids (palmitoleic acid, myristic acid, palmitic acid, and stearic acid) as the top 10 major determinants of separation (Figure 2B). The loadings plot for component 2 showed that energy metabolites (citric acid, glyceric acid, succinic acid, fucose, fumaric acid, isocitric acid, α-ketoglutarate, glucuronic acid, and parabanic acid) and amino acid valine were the top 10 major determinants of separation (Figure 2C).

Pathway analysis

Pathway analysis was conducted to assess metabolic pathways altered by LLC metastases. The identified metabolites were mapped into 56 metabolic pathways (Supplemental Table 3) according to the KEGG database.[34] Six pathways were altered significantly by LLC metastases. These 6 pathways were mainly related to amino acid and energy metabolism, namely aminoacyl-tRNA biosynthesis, arginine biosynthesis, alanine, aspartate, and glutamate metabolism, BCAA biosynthesis, glyoxylate and dicarboxylate metabolism, and citrate cycle (Table 5, Figure 3).

Network analysis

The network analysis highlights potential functional relationships among the metabolites identified. Regardless of diet, the genotype difference significantly altered 8 metabolic pathways between WT and *Mcp-1*$^{-/-}$ mice. These pathways were the citrate cycle, alanine, aspartate, and glutamate metabolism, BCAA biosynthesis, pantothenate and CoA biosynthesis, pentose phosphate pathway, glyoxylate and dicarboxylate metabolism, BCAA metabolism, and glycerolipid metabolism (Table 6). Additionally, diet, regardless of genotype, significantly altered 8 metabolic pathways between the AIN93G diet and HFD. They were glycine, serine, and threonine metabolism, glycolysis/gluconeogenesis, BCAA biosynthesis, galactose metabolism, fatty acid synthesis, glyoxylate and dicarboxylate metabolism, glutathione metabolism, and alanine, aspartate, and glutamine metabolism (Table 6). The functional relationship of the identified metabolites for genotype and diet are presented in Figure 4A and B, respectively.

Discussion

Lewis lung carcinoma is an aggressive murine carcinoma that metastasizes spontaneously to the lungs.[9,23] The present study showed that amino acid metabolism is a major metabolic alternation in LLC-bearing mice. This is evidenced by the fact that of the 6 metabolic pathways identified by the pathway analysis that are altered significantly, 4 are related to amino acid metabolism. The aminoacyl-tRNA biosynthesis pathways feature a group of enzymes that are responsible for aminoacylation of amino acids with a tRNA to form their respective amino acid-tRNA in the first step of protein translation.[36] The other 3 pathways are arginine biosynthesis, alanine, aspartate, and glutamate metabolism, and BCAA biosynthesis pathways.

Network analysis showed alterations in both BCAA biosynthesis and metabolism pathways when compared *Mcp-1*$^{-/-}$ mice to WT mice. The heatmap analysis showed that both valine and isoleucine in plasma were lower in *Mcp-1*$^{-/-}$ mice, particularly those fed the HFD. BCAAs are essential amino acids and building blocks for proteins. They activate the

Table 1. Plasma metabolites related to amino acid metabolism in Lewis lung carcinoma-bearing wild-type (WT) and *Mcp-1*$^{-/-}$ mice fed the AIN93G or high-fat diet (HFD).

	AIN93G WT	AIN93G *MCP-1*$^{-/-}$	HFD WT	HFD *MCP-1*$^{-/-}$	DIET *P*	GENE *P*	DIET × GENE *P*
N-acetylglycine	1.00 ± 0.16	1.12 ± 0.22	1.03 ± 0.21	0.74 ± 0.15	.34	.64	.28
Alanine	1.00 ± 0.07	0.89 ± 0.10	1.08 ± 0.07	1.14 ± 0.07	.04	.77	.28
Aminomalonate	1.00 ± 0.09	1.20 ± 0.09	1.26 ± 0.09	1.10 ± 0.14	.46	.81	.09
Asparagine	1.00 ± 0.10	0.95 ± 0.06	1.12 ± 0.07	1.15 ± 0.08	.06	.86	.63
Citrulline	1.00 ± 0.05	0.94 ± 0.06	1.13 ± 0.05	1.02 ± 0.06	.06	.13	.71
Creatine	1.00 ± 0.06	0.96 ± 0.10	1.03 ± 0.09	0.87 ± 0.15	.75	.32	.54
Creatinine	1.00 ± 0.06	0.95 ± 0.09	1.07 ± 0.10	0.98 ± 0.13	.60	.46	.85
Cysteine	1.00 ± 0.11	0.92 ± 0.14	1.26 ± 0.10	1.04 ± 0.12	.12	.21	.56
Cystine	1.00 ± 0.20	1.04 ± 0.15	1.03 ± 0.09	1.07 ± 0.22	.85	.82	.98
Glutamic acid	1.00 ± 0.11	1.04 ± 0.14	1.04 ± 0.09	0.99 ± 0.13	.96	.97	.69
Glutamine	1.00 ± 0.12	1.17 ± 0.22	1.27 ± 0.15	1.09 ± 0.14	.57	.97	.27
Glycine	1.00 ± 0.07	0.92 ± 0.09	1.12 ± 0.05	1.27 ± 0.12	<.01	.70	.15
Histidine	1.00 ± 0.10	1.07 ± 0.12	1.14 ± 0.11	1.03 ± 0.12	.68	.89	.43
Indole-3-lactate	1.00 ± 0.07	1.21 ± 0.11	1.29 ± 0.12	1.12 ± 0.07	.30	.87	.06
Isoleucine	1.00 ± 0.05	0.92 ± 0.05	0.91 ± 0.05	0.78 ± 0.05	.03	.04	.61
Leucine	1.00 ± 0.08	0.95 ± 0.04	0.92 ± 0.04	0.86 ± 0.05	.15	.33	.95
Lysine	1.00 ± 0.09	1.15 ± 0.11	1.11 ± 0.11	1.10 ± 0.10	.81	.50	.44
Methionine	1.00 ± 0.07	1.00 ± 0.09	1.20 ± 0.06	1.08 ± 0.09	.08	.41	.45
Methionine sulfoxide	1.00 ± 0.08	0.99 ± 0.13	1.05 ± 0.07	1.00 ± 0.07	.75	.75	.84
Ornithine	1.00 ± 0.08	1.04 ± 0.10	1.17 ± 0.11	1.11 ± 0.09	.22	.93	.58
Oxoproline	1.00 ± 0.06	1.04 ± 0.04	1.08 ± 0.04	1.20 ± 0.06	.03	.14	.46
Phenylalanine	1.00 ± 0.05	0.97 ± 0.04	0.97 ± 0.05	0.91 ± 0.03	.28	.33	.73
Proline	1.00 ± 0.13	0.87 ± 0.17	1.39 ± 0.24	0.95 ± 0.24	.25	.17	.46
Serine	1.00 ± 0.07	0.96 ± 0.11	1.18 ± 0.05	1.23 ± 0.04	<.01	.99	.53
Trans-4-hydroproline	1.00 ± 0.06	1.02 ± 0.06	1.06 ± 0.05	1.20 ± 0.07	.04	.19	.30
Threonine	1.00 ± 0.06	1.05 ± 0.12	1.24 ± 0.06	1.20 ± 0.10	.02	.98	.60
Tryptophan	1.00 ± 0.11	1.08 ± 0.09	1.13 ± 0.09	1.06 ± 0.11	.58	.99	.45
Tyrosine	1.00 ± 0.07	0.98 ± 0.10	1.15 ± 0.09	1.11 ± 0.10	.13	.76	.90
Urea	1.00 ± 0.13	1.08 ± 0.17	1.02 ± 0.16	1.16 ± 0.17	.74	.49	.85
Valine	1.00 ± 0.05	0.87 ± 0.03	0.93 ± 0.03	0.82 ± 0.05	.18	<.01	.79
2-aminobutyric acid	1.00 ± 0.09	1.00 ± 0.15	1.27 ± 0.08	1.07 ± 0.10	.11	.32	.32
2-hydroxybutanoic acid	1.00 ± 0.17	1.41 ± 0.35	0.94 ± 0.13	1.68 ± 0.56	.74	.08	.60
2-ketoisocaproic acid	1.00 ± 0.10	0.91 ± 0.08	1.00 ± 0.07	0.83 ± 0.06	.64	.11	.65

Values of treatment groups are normalized to that of the AIN93G WT group. Values are means ± SEM with false discovery rate-adjusted *P* values (n = 12 per group for WT mice, n = 10 per group for *Mcp-1*$^{-/-}$ mice).

Table 2. Plasma metabolites related to energy metabolism in Lewis lung carcinoma-bearing wild-type (WT) and *Mcp-1*$^{-/-}$ mice fed the AIN93G or high-fat diet (HFD).

	AIN93G WT	AIN93G *MCP-1*$^{-/-}$	HFD WT	HFD *MCP-1*$^{-/-}$	DIET *P*	GENE *P*	DIET × GENE *P*
α-Ketoglutarate	1.00 ± 0.08	1.24 ± 0.15	1.02 ± 0.08	1.29 ± 0.22	.79	.07	.91
Citric acid	1.00 ± 0.03	1.19 ± 0.05	0.98 ± 0.04	1.15 ± 0.10	.64	<.01	.84
Erythritol	1.00 ± 0.10	1.24 ± 0.09	1.17 ± 0.11	1.27 ± 0.05	.29	.09	.45
Fructose	1.00 ± 0.10	1.23 ± 0.10	0.88 ± 0.14	1.18 ± 0.09	.44	.02	.76
Fucose	1.00 ± 0.05	1.18 ± 0.06	1.14 ± 0.05	1.26 ± 0.06	.05	<.01	.52
Fumaric acid	1.00 ± 0.05	1.18 ± 0.09	0.94 ± 0.06	1.13 ± 0.10	.49	.01	.89
Glucose-1-phosphate	1.00 ± 0.11	1.15 ± 0.15	1.39 ± 0.12	1.46 ± 0.21	.02	.48	.77
Galactitol	1.00 ± 0.07	1.06 ± 0.10	1.38 ± 0.09	1.53 ± 0.08	<.01	.24	.60
Glycerol-α-phosphate	1.00 ± 0.05	1.05 ± 0.05	0.87 ± 0.08	0.86 ± 0.03	.01	.74	.68
Glucose	1.00 ± 0.08	1.19 ± 0.07	1.47 ± 0.08	1.49 ± 0.08	<.01	.20	.29
Glucuronic acid	1.00 ± 0.05	1.10 ± 0.08	1.03 ± 0.04	1.13 ± 0.07	.65	.11	.99
Isocitric acid	1.00 ± 0.03	1.14 ± 0.08	0.95 ± 0.04	1.10 ± 0.09	.43	.02	.95
Lactic acid	1.00 ± 0.12	0.66 ± 0.09	0.80 ± 0.16	0.82 ± 0.12	.89	.23	.18
Malic acid	1.00 ± 0.08	1.09 ± 0.13	0.95 ± 0.09	1.01 ± 0.14	.55	.50	.91
Mannose	1.00 ± 0.04	1.11 ± 0.07	1.11 ± 0.06	1.09 ± 0.03	.46	.40	.20
Methyl O-D-galactopyranoide	1.00 ± 0.11	1.07 ± 0.10	1.48 ± 0.11	1.49 ± 0.09	<.01	.72	.79
Myoinositol	1.00 ± 0.05	0.97 ± 0.05	1.20 ± 0.07	1.22 ± 0.06	<.01	.89	.73
Pyruvic acid	1.00 ± 0.15	1.01 ± 0.15	1.77 ± 0.25	1.59 ± 0.19	<.01	.64	.62
Sorbitol	1.00 ± 0.21	1.49 ± 0.20	1.49 ± 0.24	1.90 ± 0.18	.04	.04	.85
Succinic acid	1.00 ± 0.10	1.46 ± 0.12	1.06 ± 0.09	1.28 ± 0.19	.64	.01	.34
Threose	1.00 ± 0.10	1.23 ± 0.07	1.10 ± 0.07	1.06 ± 0.06	.65	.25	.08
1,5-anhydroglucitol	1.00 ± 0.05	1.05 ± 0.06	0.70 ± 0.03	0.68 ± 0.03	<.01	.69	.44
6-deoxyglucose	1.00 ± 0.04	1.07 ± 0.06	1.06 ± 0.06	1.18 ± 0.05	.11	.07	.60
6-deoxyglucitol	1.00 ± 0.09	1.26 ± 0.11	1.07 ± 0.09	0.96 ± 0.07	.22	.43	.06
Xylose	1.00 ± 0.09	1.34 ± 0.11	1.30 ± 0.13	1.32 ± 0.10	.19	.10	.14

Values of treatment groups are normalized to that of the AIN93G WT group. Values are means ±SEM with false discovery rate-adjusted *P* values (n = 12 per group for WT mice, n = 10 per group for *Mcp-1*$^{-/-}$ mice).

mammalian target of rapamycin complex (mTORC) pathway for protein synthesis, or they can be converted to glutamate, through α-ketoglutarate, which can either fuel the citrate cycle or serve as an indirect source of nitrogen for nucleotide and non-essential amino acid syntheses.[37,38] Non-small cell lung carcinoma takes up circulating BCAAs and incorporates them into tissue protein and uses it as a nitrogen source.[37] We found that LLC metastases contain a greater amount of valine when compared to the normal lung tissue.[39] In the present study, the decreased valine in *Mcp-1*$^{-/-}$ mice, particularly those fed the HFD, is consistent with a recent metabolomic analysis showing that plasma level of valine is lower in adipose-specific *Mcp-1* deficient MMTV-PyMT mice.[18] Taken together, these findings indicate that the inflammatory cytokine MCP-1 may modulate BCAA metabolism pathways in cancer-bearing mice.

Table 3. Plasma metabolites related to lipid metabolism in Lewis lung carcinoma-bearing wild-type (WT) and *Mcp-1*$^{-/-}$ mice fed the AIN93G or high-fat diet (HFD).

	AIN93G WT	AIN93G *MCP-1*$^{-/-}$	HFD WT	HFD *MCP-1*$^{-/-}$	DIET *P*	GENE *P*	DIET × GENE *P*
Arachidic acid	1.00 ± 0.11	1.18 ± 0.14	1.13 ± 0.23	1.15 ± 0.10	.76	.53	.59
Arachidonic acid	1.00 ± 0.06^{ab}	1.27 ± 0.09^{a}	0.96 ± 0.05^{ab}	0.88 ± 0.12^{b}	.01	.23	.04
Cholesterol	1.00 ± 0.08	1.11 ± 0.05	0.88 ± 0.04	0.94 ± 0.07	.02	.19	.64
Dihydrocholesterol	1.00 ± 0.11	1.29 ± 0.09	1.26 ± 0.11	1.24 ± 0.12	.32	.22	.17
Ethanolamine	1.00 ± 0.10	0.92 ± 0.07	0.85 ± 0.05	0.91 ± 0.13	.38	.90	.45
Glyceric acid	1.00 ± 0.08	1.40 ± 0.09	1.11 ± 0.07	1.49 ± 0.24	.44	<.01	.93
Glycerol	1.00 ± 0.05	1.03 ± 0.04	0.97 ± 0.04	0.93 ± 0.04	.14	.86	.44
Heptadecanoic acid	1.00 ± 0.10	1.17 ± 0.07	0.97 ± 0.09	1.04 ± 0.10	.39	.20	.59
Inositol-4-monophosphate	1.00 ± 0.19	1.22 ± 0.21	1.23 ± 020	0.96 ± 0.22	.95	.89	.23
Lauric acid	1.00 ± 0.11	1.09 ± 0.17	1.28 ± 0.17	1.26 ± 0.10	.11	.81	.71
Linoleic acid	1.00 ± 0.07	0.96 ± 0.11	1.19 ± 0.13	1.30 ± 0.25	.08	.81	.62
Myristic acid	1.00 ± 0.09	1.02 ± 0.12	0.51 ± 0.03	0.66 ± 0.10	<.01	.35	.50
Oleic acid	1.00 ± 0.20	1.02 ± 0.29	1.09 ± 0.13	1.09 ± 0.27	.71	.97	.97
Palmitic acid	1.00 ± 0.05	1.12 ± 0.07	0.78 ± 0.04	0.81 ± 0.06	<.01	.16	.42
Palmitoleic acid	1.00 ± 0.16	0.96 ± 0.12	0.23 ± 0.03	0.27 ± 0.05	<.01	.98	.74
Phosphate	1.00 ± 0.03	0.93 ± 0.05	0.99 ± 0.04	0.95 ± 0.06	.97	.19	.82
Stearic acid	1.00 ± 0.08	1.12 ± 0.08	0.81 ± 0.05	0.85 ± 0.04	<.01	.23	.54
3-hydroxybutyric acid	1.00 ± 0.18	0.97 ± 0.20	0.75 ± 0.18	0.77 ± 0.21	.24	.97	.89

Values of treatment groups are normalized to that of the AIN93G WT group. Values are means ± SEM with false discovery rate-adjusted *P* values (n = 12 per group for WT mice, n = 10 per group for *Mcp-1*$^{-/-}$ mice). Values in the same row with different letters are significant at $P \leq .05$.

Table 4. Plasma metabolites related to vitamin and nucleotide metabolism in Lewis lung carcinoma-bearing wild-type (WT) and *Mcp-1*$^{-/-}$ mice fed the AIN93G or high-fat diet (HFD).

	AIN93G WT	AIN93G *MCP-1*$^{-/-}$	HFD WT	HFD *MCP-1*$^{-/-}$	DIET *P*	GENE *P*	DIET × GENE *P*
Vitamins							
Nicotinic acid	1.00 ± 0.18	0.77 ± 0.11	0.94 ± 0.14	1.06 ± 0.24	.51	.74	.32
α-Tocopherol	1.00 ± 0.10	0.95 ± 0.12	1.08 ± 0.08	0.94 ± 0.11	.76	.36	.65
Threonic acid	1.00 ± 0.07	1.14 ± 0.12	0.95 ± 0.09	1.01 ± 0.13	.37	.32	.68
Nucleotides							
Allantoic acid	1.00 ± 0.11	1.37 ± 0.15	1.50 ± 0.09	1.42 ± 0.16	.04	.27	.09
Oxalic acid	1.00 ± 0.19	1.25 ± 0.26	0.98 ± 0.19	1.24 ± 0.30	.93	.27	.99
Parabanic acid	1.00 ± 0.18	1.34 ± 0.28	0.80 ± 0.09	1.51 ± 0.35	.95	.03	.43
Pseudouridine	1.00 ± 0.06	1.14 ± 0.12	1.34 ± 0.08	1.29 ± 0.04	<.01	.54	.26
Ribose	1.00 ± 0.06	1.20 ± 0.22	1.18 ± 0.14	1.62 ± 0.10	.03	.02	.40
Thymidine	1.00 ± 0.07	0.94 ± 0.07	1.14 ± 0.08	0.97 ± 0.11	.33	.18	.48
Uracil	1.00 ± 0.12	0.84 ± 0.12	1.08 ± 0.08	0.68 ± 0.13	.72	.02	.29
Uric acid	1.00 ± 0.08	1.18 ± 0.13	1.17 ± 0.05	1.19 ± 0.05	.30	.24	.32

Values of treatment groups are normalized to that of the AIN93G WT group. Values are means ± SEM with false discovery rate-adjusted *P* values (n = 12 per group for WT mice, n = 10 per group for *Mcp-1*$^{-/-}$ mice).

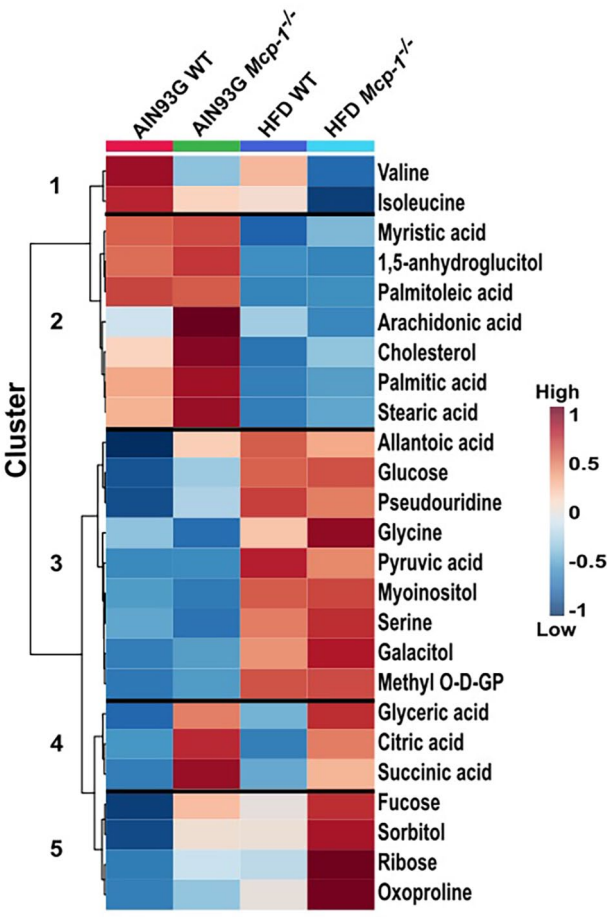

Figure 1. Twenty-five metabolites identified by the hierarchical clustering heatmap analysis in plasma that differed most in wild-type (WT) and *Mcp-1*$^{-/-}$ mice fed the AIN93G or high-fat diet (HFD). AIN93G WT (red): WT mice fed the AIN93G diet; AIN93G *Mcp-1*$^{-/-}$ (green): *Mcp-1*$^{-/-}$ mice fed the AIN93G diet; HFD WT (blue): WT mice fed the HFD; HFD *Mcp-1*$^{-/-}$ (cyan): *Mcp-1*$^{-/-}$ mice fed the HFD (n = 12 per group for WT mice, n = 10 per group for *Mcp-1*$^{-/-}$ mice). Methyl O-D-GP: Methyl O-D-galactopyranoside.

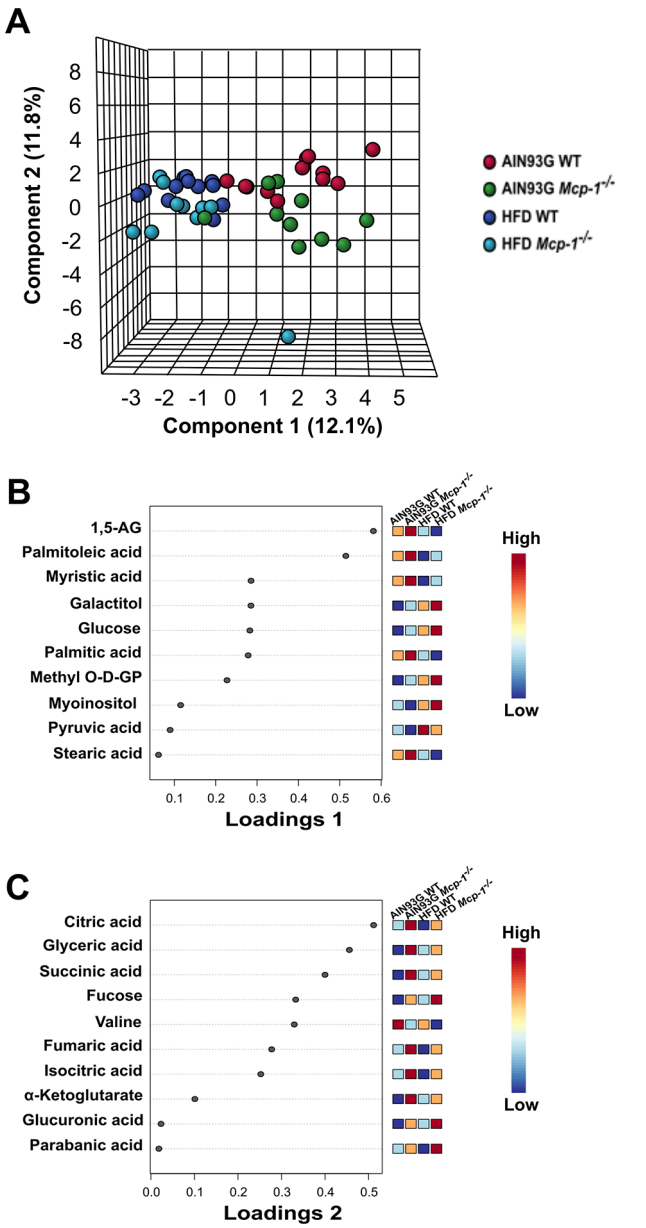

Figure 2. Components 1 and 2 of the synchronized 3-dimensional plot (A) by spare partial least square-discriminant analysis (sPLS-DA) of plasma metabolites from wild-type (WT) and *Mcp-1*$^{-/-}$ mice fed the AIN93G or high-fat diet (HFD) and loading plots of the most influential 10 metabolites in treatment separation among the 4 dietary groups for components 1 (B) and 2 (C). AIN93G WT (red): WT mice fed the AIN93G diet; AIN93G *Mcp-1*$^{-/-}$ (green): *Mcp-1*$^{-/-}$ mice fed the AIN93G diet; HFD WT (blue): WT mice fed the HFD; HFD *Mcp-1*$^{-/-}$ (cyan): *Mcp-1*$^{-/-}$ mice fed the HFD (n = 12 per group for WT mice, n = 10 per group for *Mcp-1*$^{-/-}$ mice). 1,5-AG: 1,5-anhydroglucitol; Methyl O-D-GP: methyl O-D-galactopyranoside.

Elevations of plasma serine and glycine in mice fed the HFD indicate that the HFD may alter serine and glycine metabolism in LLC-bearing mice. Serine is a commonly consumed metabolite by cancer cells.[40,41] A significant amount of serine is converted to glycine by hydromethyltransferases in cancer cells.[42,43] Elevation of glycine occurs in breast cancer patients with lower survival rates.[44] Dietary serine and glycine starvation reduces tumorigenesis in murine models of lymphoma and intestinal cancer.[45] The observed serine and glycine elevations along with the elevation of glucose may contribute, at least partly, to the HFD-enhanced metastatic growth in the lungs.[9]

The network analysis showed that the HFD altered the fatty acid synthesis pathway in LLC-bearing mice. The clustered heatmap analysis showed that the HFD, compared to the AIN93G diet, lowered arachidonic acid (20:4) in plasma. Arachidonic acid can be obtained from the diet by desaturation and elongation of dietary linoleic acid.[46,47] It has been reported that arachidonic acid and its metabolite 20-hydroxyeicosatetraenoic acid (20-HETE) are carcinogenic in laboratory rodents.[48,49] The 20-HETE can activate multiple signal pathways in cancer, including intracellular protein kinases and chemokines.[50,51] Alterations in arachidonic acid metabolism have been reported in human cancer

Table 5. Metabolic pathways identified by the pathway analysis that are significantly altered by Lewis lung carcinoma metastasis.

KEGG PATHWAY	NUMBER OF METABOLITES IDENTIFIED	P[A]	IMPACT[B]
Aminoacyl-tRNA biosynthesis	18	<.01	0.17
Arginine biosynthesis	7	<.01	0.41
Alanine, aspartate and glutamate metabolism	9	<.01	0.36
Valine, leucine and isoleucine biosynthesis	5	<.01	0
Glyoxylate and dicarboxylate metabolism	8	.01	0.26
Citrate cycle	6	.03	0.30

[a]*P* values are obtained by the over-representation analysis and adjusted by the Holm method.
[b]Impact is the pathway impact score obtained by the pathway topology analysis.

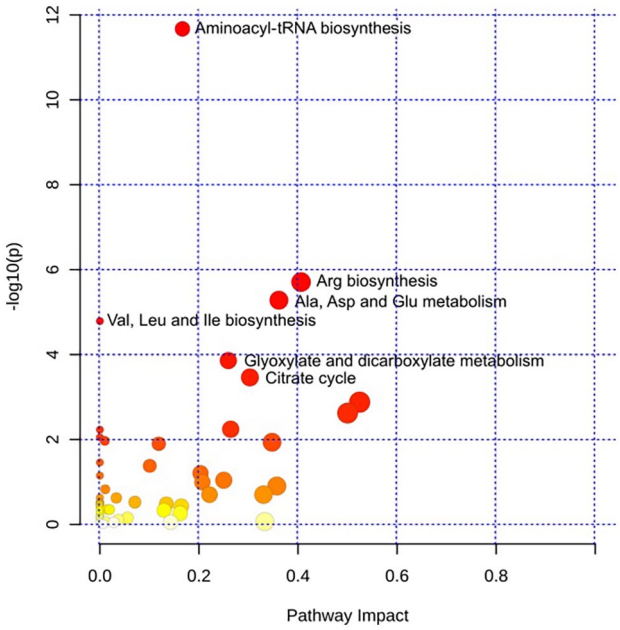

Figure 3. Matched metabolic pathway plot of metabolites identified in plasma from wild-type (WT) and *Mcp-1*$^{-/-}$ mice fed the AIN93G or high-fat diet. The *x*-axis marks the pathway impact and the *y*-axis marks the pathway enrichment. Each node represents a pathway. The nodes with larger sizes and darker colors (from yellow to red) positioning toward top right region represent higher pathway impact values and higher pathway enrichment. Pathways that are significantly altered are presented with their names next to their nodes. All detected metabolic pathways are presented in Supplemental Table 3.

patients[52] and cancer models in laboratory rodents.[53] Our findings suggest the possibility of an accelerated utilization of arachidonic acid during the HFD-enhanced metastatic progression. It warrants further investigation of arachidonic acid metabolism in the presence of malignancy, particularly the involvement of fatty acid desaturases in its conversion from linoleic acid and its metabolism to 20-HETE.

Table 6. Metabolic pathways identified by the network analysis that are significantly altered by genotype (wild-type vs. *Mcp-1*$^{-/-}$) and diet (AIN93G vs. high-fat diet) in Lewis lung carcinoma-bearing wild-type and *Mcp-1*$^{-/-}$ mice fed the AIN93G or high-fat diet.

METABOLIC PATHWAYS	HITS	*P*
Wild-type mice versus *Mcp-1*$^{-/-}$ mice		
Citrate cycle	3	<.01
Alanine, aseparate, and glutamate metabolism	3	<.01
Valine, leucine, and isoleucine biosynthesis	2	<.01
Pantothenate and CoA biosynthesis	2	<.01
Pentose phosphate pathway	2	.01
Glyoxylate and dicarboxylate metabolism	2	.02
Valine, leucine, and isoleucine metabolism	2	.03
Glycerolipid metabolism	1	.05
Arginine biosynthesis	1	.10
AIN93G diet versus high-fat diet		
Glycine, serine, and threonine metabolism	4	<.01
Glycolysis/gluconeogenesis	3	<.01
Valine, leucine, and isoleucine biosynthesis	2	<.05
Galactose metabolism	3	<.01
Fatty acid synthesis	2	<.01
Glyoxylate and dicarboxylate metabolism	3	<.01
Glutathione metabolism	2	.02
Alanine, aspartate, and glutamate metabolism	2	.05
Cysteine and methionine metabolism	2	.07

Compared to the AIN93G diet, the HFD lowered cholesterol and long-chain saturated fatty acids [myristic acid (14:0), palmitic acid (16:0), and stearic acid (18:0)] in plasma. It has been shown that the incorporation of cholesterol in cell membrane reduces fluidity and consequently cell dissemination by limiting cell morphologic changes during intravasation and extravasation of metastasis.[54] Furthermore, elevated *de novo* synthesis of saturated and monounsaturated fatty acids in cancer cells makes membranes more stable than polyunsaturated fatty acids, which may protect cancer cells against oxidative stress.[55] The HFD enhances metastasis.[9] Thus, whether the observed lowering in cholesterol and long-chain saturated fatty acids contribute to HFD-enhanced metastasis through alteration in membrane fluidity during metastatic dissemination warrants further investigation.

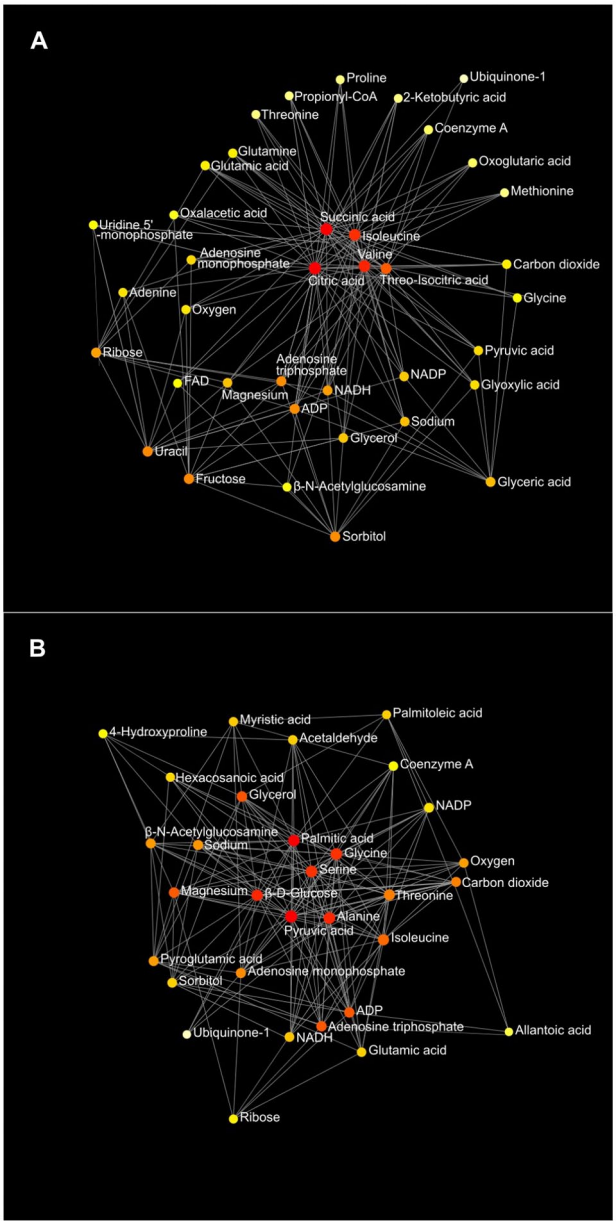

Figure 4. Metabolic network of the identified metabolites between wild-type and *Mcp-1*$^{-/-}$ mice (A) and between the AIN93G and high-fat diet (B). Colors, from white-yellow to red, indicate levels of impact the metabolites have to the network in an ascending order (the number of connections a node has to other nodes and the number of shortest paths going through the node). Network statistics for analyses A and B are presented in Table 6.

The HFD may have shifted energy production away from mitochondrial ATP production and toward glycolysis in LLC-bearing mice. The elevated plasma glucose and pyruvic acid and a lower content of 1,5-anhydroglucitol (a marker of glycemic control[56]) in HFD-fed mice suggest impaired utilization of glucose. Cancer cells increase their glucose uptake to meet their high energy demand through aerobic glycolysis for anabolism.[57,58] The notion that the HFD accelerates glycolysis in LLC-bearing mice is supported by findings from a recent metabolomic comparison in which elevated glucose and decreased 1,5-anhydroglucitol occur in plasma from MMTV-PyMT mice fed a HFD.[18]

In the present study, we observed elevations of citric acid, fumaric acid, isocitric acid, succinic acid, and glyceric acid in *Mcp-1*$^{-/-}$ mice regardless of the diet. Furthermore, the network analysis showed alteration in the citrate cycle pathway when compared *Mcp-1*$^{-/-}$ mice to WT mice. Citric acid, fumaric acid, isocitric acid, and succinic acid are metabolic intermediates of the citrate cycle. Glyceric acid is an oxidative product of glycerol; its phosphate derivatives are important intermediates of glycolysis.[59] Taken together, the elevated expression of citrate cycle intermediates suggests metabolic alteration in mitochondria in *Mcp-1*$^{-/-}$ mice. However, it does not exclude the possibility of a compensatory elevation in the absence of MCP-1 as increased plasma concentrations proinflammatory cytokines and angiogenic factors occur in these *Mcp-1*$^{-/-}$ mice.[9]

The heatmap analysis showed that sorbitol, fucose, ribose, and oxoproline contents were higher in HFD-fed *Mcp-1*$^{-/-}$ mice compared to other groups. Sorbitol is a sugar alcohol. It can be obtained from diets or derived endogenously from glucose by aldose reductase and converted to fructose by sorbitol dehydrogenase in cells.[60,61] The elevated expression of fructose is consistence with the elevation of sorbitol and suggests the altered sorbitol metabolism in *Mcp-1*$^{-/-}$ mice. Fucose (a monosaccharide) is a constituent of N-glycans. Ribose is a component of ribonucleotide from which RNA is built. Oxoproline (an amino acid derivative) is a metabolite of the glutathione cycle that detoxifies hydrogen peroxide. The MCP-1 deficiency mitigates malignant spread of LLC in mice fed the HFD, indicating the involvement of MCP-1 in HFD-enhanced metastasis.[9] The observed elevations of the aforementioned metabolites suggest an interaction between HFD and MCP-1 deficiency, because such elevations were not found in other groups. Thus, the roles of these metabolites and their related metabolic pathways in HFD-enhanced metastasis, particularly their interactions with MCP-1, remains to be an interest for further investigation.

Limitations of this study are that we were not able to perform metabolomic analysis on LLC metastases (the entire lungs were fixed to examine the extent of metastasis) nor had plasma samples from non-LLC-bearing mice fed different diets as negative controls. These limitations made us unable to conduct parallel comparisons of metabolomic differences between the metastases and plasma nor differences between the presence and absence of metastasis. Nevertheless, this study for the first time presented plasma metabolome in mice bearing LLC lung metastases and their alterations resulted from *Mcp-1*$^{-/-}$ knockout.

In summary, LLC metastases altered the amino acid metabolism considerably. The HFD altered lipid and energy metabolism in mice bearing LLC lung metastases. Elevations in citrate cycle intermediates in *Mcp-1*$^{-/-}$ mice indicates the involvement

of MCP-1 in mitochondrial energy metabolism during LLC malignant spread. Findings from this study can be helpful understanding the impact of obesity on prevention and treatment of metastasis.

Acknowledgement

The authors gratefully acknowledge Dr. Kathleen Yeater (Plains Area Administrative Office, Agricultural Research Service) for assistance in statistical analysis and the following staff of the Grand Forks Human Nutrition Research Center: Lana DeMars and Jack He for technical support and vivarium staff for making animal diets and providing high-quality animal care. USDA is an equal opportunity provider and employer. Mention of trade names or commercial products in this publication is solely for the purpose of providing specific information and does not imply recommendation or endorsement by the USDA.

Author Contributions

LY and SS designed the study, conducted experiments, and collected data. All authors contributed to data analysis, result interpretation, and wrote and revised the manuscript.

Ethics Statement

The Institutional Animal Care and Use Committee of the Grand Forks Human Nutrition Research Center, USDA ARS, reviewed and approved this study.

Supplemental Material

Supplemental material for this article is available online.

REFERENCES

1. Robinson EA, Yoshimura T, Leonard EJ, et al. Complete amino acid sequence of a human monocyte chemoattractant, a putative mediator of cellular immune reactions. *Proc Natl Acad Sci USA*. 1989;86:1850-1854.
2. Carr MW, Roth SJ, Luther E, Rose SS, Springer TA. Monocyte chemoattractant protein 1 acts as a T-lymphocyte chemoattractant. *Proc Natl Acad Sci USA*. 1994;91:3652-3656.
3. Lebrecht A, Grimm C, Lantzsch T, et al. Monocyte chemoattractant protein-1 serum levels in patients with breast cancer. *Tumour Biol*. 2004;25:14-17.
4. Lu Y, Cai Z, Galson DL, et al. Monocyte chemotactic protein-1 (MCP-1) acts as a paracrine and autocrine factor for prostate cancer growth and invasion. *Prostate*. 2006;66:1311-1318.
5. Yoshidome H, Kohno H, Shida T, et al. Significance of monocyte chemoattractant protein-1 in angiogenesis and survival in colorectal liver metastases. *Int J Oncol*. 2009;34:923-930.
6. Fang WB, Yao M, Brummer G, et al. Targeted gene silencing of CCL2 inhibits triple negative breast cancer progression by blocking cancer stem cell renewal and M2 macrophage recruitment. *Oncotarget*. 2016;7:49349-49367.
7. Nam JS, Kang MJ, Suchar AM, et al. Chemokine (C-C motif) ligand 2 mediates the prometastatic effect of dysadherin in human breast cancer cells. *Cancer Res*. 2006;66:7176-7184.
8. Cranford TL, Velázquez KT, Enos RT, et al. Loss of monocyte chemoattractant protein-1 expression delays mammary tumorigenesis and reduces localized inflammation in the C3(1)/SV40Tag triple negative breast cancer model. *Cancer Biol Ther*. 2017;18:85-93.
9. Yan L, Sundaram S. Monocyte chemotactic protein-1 deficiency reduces spontaneous metastasis of Lewis lung carcinoma in mice fed a high-fat diet. *Oncotarget*. 2016;7:24792-24799.
10. Huber J, Kiefer FW, Zeyda M, et al. CC chemokine and CC chemokine receptor profiles in visceral and subcutaneous adipose tissue are altered in human obesity. *J Clin Endocrinol Metab*. 2008;93:3215-3221.
11. Bruun JM, Lihn AS, Pedersen SB, Richelsen B. Monocyte chemoattractant protein-1 release is higher in visceral than subcutaneous human adipose tissue (AT): implication of macrophages resident in the AT. *J Clin Endocrinol Metab*. 2005;90:2282-2289.
12. Christiansen T, Richelsen B, Bruun JM. Monocyte chemoattractant protein-1 is produced in isolated adipocytes, associated with adiposity and reduced after weight loss in morbid obese subjects. *Int J Obes*. 2005;29:146-150.
13. Daniell HW. Increased lymph node metastases at mastectomy for breast cancer associated with host obesity, cigarette smoking, age, and large tumor size. *Cancer*. 1988;62:429-435.
14. Loi S, Milne RL, Friedlander ML, et al. Obesity and outcomes in premenopausal and postmenopausal breast cancer. *Cancer Epidemiol Biomarkers Prev*. 2005;14:1686-1691.
15. Bassett WW, Cooperberg MR, Sadetsky N, et al. Impact of obesity on prostate cancer recurrence after radical prostatectomy: data from CaPSURE. *Urology*. 2005;66:1060-1065.
16. Amling CL, Riffenburgh RH, Sun L, et al. Pathologic variables and recurrence rates as related to obesity and race in men with prostate cancer undergoing radical prostatectomy. *J Clin Oncol*. 2004;22:439-445.
17. Sundaram S, Yan L. Adipose monocyte chemotactic protein-1 deficiency reduces high-fat diet-enhanced mammary tumorigenesis in MMTV-PyMT mice. *J Nutr Biochem*. 2020;77:108313.
18. Yan L, Sundaram S, Rust BM, Picklo MJ, Bukowski MR. Mammary tumorigenesis and metabolome in male adipose specific monocyte chemotactic protein-1 deficient MMTV-PyMT mice fed a High-Fat diet. *Front Oncol*. 2021;11:667843.
19. Sundaram S, Yan L. Adipose-specific monocyte chemotactic protein-1 deficiency reduces pulmonary metastasis of Lewis lung carcinoma in mice. *Anticancer Res*. 2019;39:1729-1738.
20. Rull A, Escolà-Gil JC, Julve J, et al. Deficiency in monocyte chemoattractant protein-1 modifies lipid and glucose metabolism. *Exp Mol Pathol*. 2007;83:361-366.
21. Luciano-Mateo F, Cabré N, Fernández-Arroyo S, et al. Chemokine (C-C motif) ligand 2 gene ablation protects low-density lipoprotein and paraoxonase-1 double deficient mice from liver injury, oxidative stress and inflammation. *Biochim Biophys Acta Mol Basis Dis*. 2019;1865:1555-1566.
22. Luciano-Mateo F, Cabré N, Fernández-Arroyo S, et al. Chemokine C-C motif ligand 2 overexpression drives tissue-specific metabolic responses in the liver and muscle of mice. *Sci Rep*. 2020;10:11954.
23. Brodt P. Characterization of two highly metastatic variants of Lewis lung carcinoma with different organ specificities. *Cancer Res*. 1986;46:2442-2448.
24. Institute for Laboratory Animal Research. *Guide for the Care and Use of Laboratory Animals*. 8th ed. National Academies Press; 2011.
25. Fiehn O, Garvey WT, Newman JW, Lok KH, Hoppel CL, Adams SH. Plasma metabolomic profiles reflective of glucose homeostasis in non-diabetic and type 2 diabetic obese African-American women. *PLoS One*. 2010;5:e15234.
26. Piccolo BD, Keim NL, Fiehn O, Adams SH, Van Loan MD, Newman JW. Habitual physical activity and plasma metabolomic patterns distinguish individuals with low vs. High weight loss during controlled energy restriction. *J Nutr*. 2015;145:681-690.
27. Fiehn O, Wohlgemuth G, Scholz C. Setup and annotation of metabolomic experiments by integrating biological and mass spectrometric metadata. In: Ludäscher B, Raschid L, eds. *Data Integration in the Life Sciences*. Vol. 3615. Springer; 2005;224-239.
28. Kanehisa M, Goto S. KEGG: kyoto encyclopedia of genes and genomes. *Nucleic Acids Res*. 2000;28:27-30.
29. Kanehisa M. Toward understanding the origin and evolution of cellular organisms. *Protein Sci*. 2019;28:1947-1951.
30. Wishart DS, Feunang YD, Marcu A, et al. HMDB 4.0: the human metabolome database for 2018. *Nucleic Acids Res*. 2018;46:D608-D617.
31. Xia J, Wishart DS. Using MetaboAnalyst 3.0 for Comprehensive Metabolomics Data Analysis. *Curr Protoc Bioinf*. 2016;55:14.10.1-14.10.91.
32. van den Berg RA, Hoefsloot HC, Westerhuis JA, Smilde AK, van der Werf MJ. Centering, scaling, and transformations: improving the biological information content of metabolomics data. *BMC Genomics*. 2006;7:142.
33. Xia J, Wishart DS. MetPA: a web-based metabolomics tool for pathway analysis and visualization. *Bioinformatics*. 2010;26:2342-2344.
34. Kanehisa M, Furumichi M, Tanabe M, Sato Y, Morishima K. KEGG: new perspectives on genomes, pathways, diseases and drugs. *Nucleic Acids Res*. 2017;45:D353-D361.
35. Holm SA. A simple sequentially rejective multiple test procedure. *Scand J Stat*. 1979;6:65-70.
36. Rubio Gomez MA, Ibba M. Aminoacyl-trna synthetases. *RNA*. 2020;26:910-936.
37. Mayers JR, Torrence ME, Danai LV, et al. Tissue of origin dictates branched-chain amino acid metabolism in mutant Kras-driven cancers. *Science*. 2016;353:1161-1165.

38. Ananieva EA, Wilkinson AC. Branched-chain amino acid metabolism in cancer. *Curr Opin Clin Nutr Metab Care*. 2018;21:64-70.
39. Yan L, Sundaram S, Rust BM, Picklo MJ, Bukowski MR. Metabolomes of Lewis lung carcinoma metastases and normal lung tissue from mice fed different diets. *J Nutr Biochem*. 2022;107:109051. doi:10.1016/j.jnutbio.2022.109051
40. Dolfi SC, Chan LL, Qiu J, et al. The metabolic demands of cancer cells are coupled to their size and protein synthesis rates. *Cancer Metab*. 2013;1:20.
41. Jain M, Nilsson R, Sharma S, et al. Metabolite profiling identifies a key role for glycine in rapid cancer cell proliferation. *Science*. 2012;336:1040-1044.
42. Maddocks OD, Berkers CR, Mason SM, et al. Serine starvation induces stress and p53-dependent metabolic remodelling in cancer cells. *Nature*. 2013;493:542-546.
43. Tedeschi PM, Johnson-Farley N, Lin H, et al. Quantification of folate metabolism using transient metabolic flux analysis. *Cancer Metab*. 2015;3:6.
44. Giskeødegård GF, Lundgren S, Sitter B, et al. Lactate and glycine-potential MR biomarkers of prognosis in estrogen receptor-positive breast cancers. *NMR Biomed*. 2012;25:1271-1279.
45. Maddocks ODK, Athineos D, Cheung EC, et al. Modulating the therapeutic response of tumours to dietary serine and glycine starvation. *Nature*. 2017;544:372-376.
46. Komprda T, Zelenka J, Fajmonová E, Fialová M, Kladroba D. Arachidonic acid and long-chain n-3 polyunsaturated fatty acid contents in meat of selected poultry and fish species in relation to dietary fat sources. *J Agric Food Chem*. 2005;53:6804-6812.
47. Abedi E, Sahari MA. Long-chain polyunsaturated fatty acid sources and evaluation of their nutritional and functional properties. *Food Sci Nutr*. 2014;2:443-463.
48. Borin TF, Shankar A, Angara K, et al. HET0016 decreases lung metastasis from breast cancer in immune-competent mouse model. *PLoS One*. 2017;12:e0178830.
49. Arbab AS, Shankar A, Borin T, et al. Combination of vatalanib and a 20-HETE synthesis inhibitor results in decreased tumor growth in an animal model of human glioma. *Onco Targets Ther*. 2016;9:1205-1219.
50. Borin TF, Angara K, Rashid MH, Achyut BR, Arbab AS. Arachidonic acid metabolite as a novel therapeutic target in breast cancer metastasis. *Int J Mol Sci*. 2017;18:2661.
51. Yu W, Chen L, Yang YQ, et al. Cytochrome P450 ω-hydroxylase promotes angiogenesis and metastasis by upregulation of VEGF and MMP-9 in non-small cell lung cancer. *Cancer Chemother Pharmacol*. 2011;68:619-629.
52. Markin PA, Brito A, Moskaleva N, et al. Plasma metabolomic profile in prostatic intraepithelial neoplasia and prostate cancer and associations with the prostate-specific antigen and the Gleason score. *Metabolomics*. 2020;16:74.
53. Ge S, Zhou H, Zhou Z, Liu L, Lou J. Serum metabolite profiling of a 4-Nitroquinoline-1-oxide-induced experimental oral carcinogenesis model using gas chromatography-mass spectrometry. *PeerJ*. 2021;9:e10619.
54. Zhao W, Prijic S, Urban BC, et al. Candidate antimetastasis drugs suppress the metastatic capacity of breast cancer cells by reducing membrane fluidity. *Cancer Res*. 2016;76:2037-2049.
55. Rysman E, Brusselmans K, Scheys K, et al. De novo lipogenesis protects cancer cells from free radicals and chemotherapeutics by promoting membrane lipid saturation. *Cancer Res*. 2010;70:8117-8126.
56. Selvin E, Rynders GP, Steffes MW. Comparison of two assays for serum 1,5-anhydroglucitol. *Clin Chim Acta*. 2011;412:793-795.
57. Warburg O. On the origin of cancer cells. *Science*. 1956;123:309-314.
58. Liberti MV, Locasale JW. Correction to: 'The Warburg Effect: How Does it Benefit Cancer Cells?'. *Trends Biochem Sci*. 2016;41:287-218.
59. Kolb V, Orgel LE. Phosphorylation of glyceric acid in aqueous solution using trimetaphosphate. *Orig Life Evol Biosph*. 1996;26:7-13.
60. Greene DA, Chakrabarti S, Lattimer SA, Sima AA. Role of sorbitol accumulation and myo-inositol depletion in paranodal swelling of large myelinated nerve fibers in the insulin-deficient spontaneously diabetic bio-breeding rat. Reversal by insulin replacement, an aldose reductase inhibitor, and myo-inositol. *J Clin Investig*. 1987;79:1479-1485.
61. He J, Gao HX, Yang N, et al. The aldose reductase inhibitor epalrestat exerts nephritic protection on diabetic nephropathy in db/db mice through metabolic modulation. *Acta Pharmacol Sin*. 2019;40:86-97.